Asymmetric beam shaping of a diode-bar laser for multipass pumping of a thin-crystal laser

Bryn Jeffries

Clarendon Laboratory, University of Oxford, Oxford OX1 3PU, United Kingdom

David W. Coutts

Centre for Lasers and Applications, Division of Information and Communication Sciences, Macquarie University, Sydney, New South Wales 2109, Australia

Received November 1, 2004; revised manuscript received March 20, 2005; accepted May 4, 2005

Two-mirror beam shaping of a 94% fill-factor laser diode bar was investigated. We show that optimal output for the purposes of end pumping was achieved by configuring the beam shaper to reformat the single row of 60 emitters into an array containing several emitters in each row. A 15×4 output configuration was used to end pump a Yb:S-FAP laser. A nearly on-axis multipass pumping system was developed to demonstrate how the asymmetry of the beam-shaped pump source can be exploited. © 2005 Optical Society of America

OCIS codes: 140.2010, 140.3070, 140.3300, 140.3480, 140.3580, 140.5560.

1. INTRODUCTION

Laser diodes are well suited to pumping solid-state lasers because of their efficient operation and narrow bandwidth. Pump powers can be scaled beyond the limits of a single emitter by using the combined output of an array of emitters in a laser diode bar. Unfortunately the diode bars are fabricated such that the M^2 values for each emitter combine in the direction of worst beam quality, so that the focused output becomes extremely elliptical. The low beam quality of a diode bar makes it a poor pump source for three- and quasi-four-level lasers, for which end pumping is preferable. Numerous techniques exist for reformatting the output to produce equalized M^2 parameters.[1–6] One particularly simple system is the two-mirror beam-shaping system devised by Clarkson and Hanna,[1] in which the row of emitters is optically transformed into some other array. This system can be easily configured for any desired output arrangement.

For low fill-factor diodes the two-mirror beam-shaping system is best configured to convert the row of emitters into a single column, so that there is no dead space between emitters to reduce brightness. Beam shaping introduces losses that increase with the number of rows produced. Hence for bars with many emitters and high fill factors it becomes more practical to produce fewer rows and more columns. Although the M_x^2 and M_y^2 values will not be equal, a circular spot can still be produced over the length of a crystal for a suitable choice of optics.

We present here an investigation into the beam shaping of a diode bar with a high (94%) fill factor for use as a pump source for an end-pumped laser system. We show that an asymmetric shaping configuration provides a practical compromise between improved beam quality and increased transmission loss. This shaped output was used to pump a Yb:S-FAP laser, and we demonstrate a multipass pumping system that improved the pumping efficiency with this asymmetrically shaped pump source.

2. BEAM SHAPING OF A HIGH FILL-FACTOR DIODE BAR

Pumping efficiency is strongly affected by the brightness (or radiant intensity) of the pump source. The brightness for a diode laser, assuming small angles, may be written in terms of the laser's beam quality parameters M_x^2 and M_y^2 as

$$B = (\pi/4\lambda)^2 \frac{P}{M_x^2 M_y^2}, \tag{1}$$

where P is the pump power and λ is the pump wavelength. If a laser crystal is pumped with such a diode, using an optical arrangement with power transmission T, the brightness of the pump at the crystal is then given by $B=(\pi/4\lambda)^2 P\times F$, where F is a figure of merit for the system given by

$$F = \frac{T}{M_x^2 M_y^2}. \tag{2}$$

A single diode emitter in a diode-bar array has typical values of $M_y^2 \sim 1$ and $M_x^2 \approx 25$, hence we would expect that, under a lossless optical system, $F \approx 0.04$. Fan and Sanchez[7] found that the pump efficiency in an end-pumped laser system depended upon the larger of the two

M^2 values: A pump source is only as good as its worst beam quality parameter. Hence an effective figure of merit can be given by

$$F' = T(M^2_{\text{worst}})^2, \tag{3}$$

where M^2_{worst} is the larger of the two M^2 values. In this context it is easy to see why a diode bar makes for a poor end-pump source, with its typical aggregate values of $M_y^2 \sim 1$ and $M_x^2 \sim 1500$ giving a value of $F' = 10^{-6}$.

A beam-shaping system such as the two-mirror system allows the beam qualities to be altered to improve the effective brightness $B' = (\pi/4\lambda)^2 PF'$ of the diode. If a diode bar consists of a single row of i emitters with individual M^2 values m_x^2 and m_y^2, the shaper can rearrange the output to some new array of j rows and i/j columns. Consequently the aggregate M^2 values are transformed from $M_x^2 = im_x^2$, $M_y^2 = m_y^2$ to $M_x^2 = (i/j)m_x^2$, $M_y^2 = jm_y^2$. This allows F' to be reduced even though the original figure of merit F remains invariant.

A typical diode bar has a single row of ~20 emitters, so F' is maximized by reformatting its output into a single column ($j = i$). A further gain is made in doing so because dead space between emitters is removed. In some bars dead space can take up to as much as 50% of the emitter area, so its removal can provide a factor of 2 improvement in brightness. In practice some dead space will be added between each row of output from the shaper. Furthermore the transmission through the shaper will decrease with the number of output rows from clipping and reflection losses. Other detrimental effects such as axial mode shift also become significant for large numbers of rows, as the path difference between the top and the bottom row becomes comparable to the confocal parameter for the focused output from a single row of emitters.

For a low fill-factor diode bar these losses are outweighed by the removal of dead space. With one exception,[8] the two-mirror beam-shaping systems reported in the literature[9–11] appear to have been configured to produce a single column of output.

As the fill factor increases, and the diode looks more like a continuous line source, beam shaping is likely to introduce more dead space than is removed. Hence the prime objective is to reduce the M^2_{worst} while keeping transmission losses to a minimum. An optimal configuration for the shaper may then require several emitters in each row of output. To demonstrate the benefits of such a configuration, we compared the effective figures of merit for a beam-shaped diode bar when the beam shaper was configured for three different output arrangements.

3. BEAM-SHAPING EXPERIMENTS

We used a two-mirror beam-shaping system constructed in-house to improve the output format of a Coherent B1-91-90.0P-60-90-A laser diode bar. The bar consisted of 60 emitters in a single 1 cm wide row, with a fast-axis microlens attached. The emitters were incoherent with one another. Figure 1 shows the output profile of the diode bar imaged onto a CCD camera, with different x and y magnifications.

In the emitter array plane ($x-z$) each emitter was approximately 150 μm wide, with an emitter pitch of 160 μm that gave the bar a 94% fill factor. The bar had an angular divergence in this plane of $\theta_x = 10°$, giving each emitter a beam quality value of $M_x^2 = 26$, or 28 inclusive of dead space.

In the diode junction plane ($y-z$) each emitter was 1 μm thick and so output should have been near-diffraction limited. Observations of the far-field beam profile from the diode in the junction plane showed that non-Gaussian structure was present in the output. It can be seen from Fig. 1 that smile was present in the diode output, such that the emitter faces occupied a rectangular region 55% larger than a completely straight row of emitters. The smile limited the minimum spacing possible between the rows of output from the shaper without losing light, and so increased the effective M_y^2 of the bar. A method exists[12] to reduce the smile in the output from a diode bar, but it was not used in our system during these experiments.

Figure 2 shows the layout of the beam-shaping system. Cylindrical optics allowed us to work with the diode output in the x and y directions independently. Shaping is most effective if emitters are imaged at the position of the beam-shaper mirrors so that the edges are well defined and the input aperture can be filled without reducing throughput. Hence in the x axis the emitters were imaged into the shaper by a pair of cylindrical lenses (CL1 and CL3). In the y axis the poor quality of the far-field output from the diode bar forced us to collimate the diode output into the shaper (using lens CL2 in combination with the microlens ML) so as to avoid producing two lobes at the pump spot focus. The diode output had approximate dimensions at the shaper of 27 and 1 mm in the x and y directions, respectively.

The beam shaper (BS in Fig. 2) reformatted the output of the laser diode bar from a single row of emitters into an array containing several rows of emitters. The shaped output was brought to a spot with a combination of a spherical achromat (SA1) and a cylindrical lens (CL4) as shown. The focal lengths and positions of the two lenses were chosen to produce a circular spot at focus, suitable for end pumping a laser crystal.

We found upon examining the polarization of the pump spot that some depolarization was incurred by the diode-bar output as it passed through the beam shaper. The incoming (horizontally polarized) diode radiation underwent incremental polarization phase shifts in the

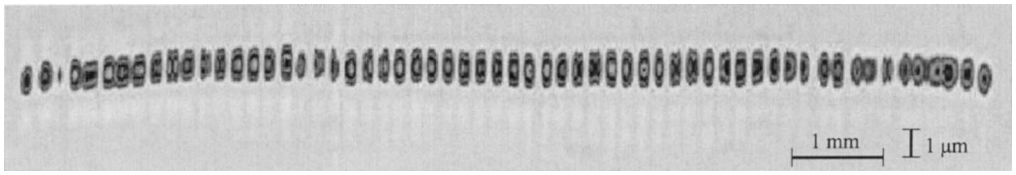

Fig. 1. Image of diode emitters with approximate dimensions. The x and y magnifications are unequal.

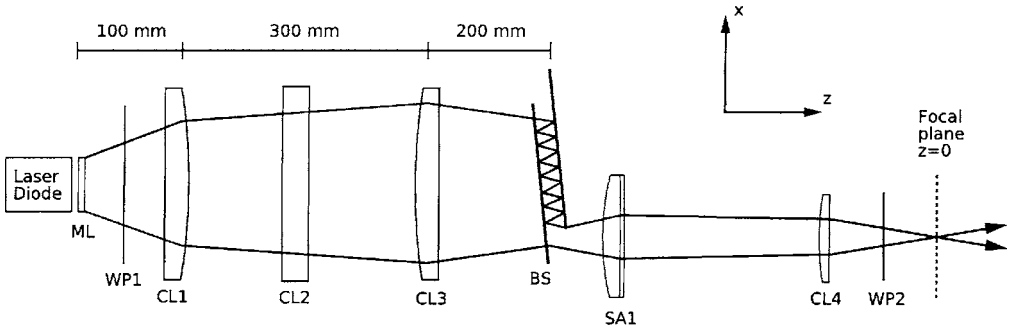

Fig. 2. Plan view of diode-bar beam-shaping setup. The diode output is imaged at the beam shaper BS in the $x-z$ plane with cylindrical lenses CL1 ($f=100$ mm) and CL3 ($f=200$ mm), and collimated in the $y-z$ plane by the microlens ML and CL2 ($f=76.5$ mm). The shaped output is brought to a spot by spherical achromat SA1 ($f=200$ mm) and CL4 ($f=50$ mm). Wave plates WP1 and WP2 were added to preserve polarization through the shaper.

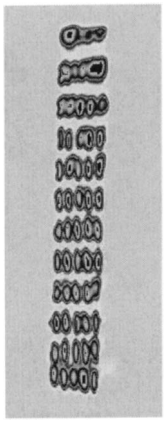

Fig. 3. CCD image of the emitters after beam shaping into a 12×5 configuration.

dielectric mirror coatings at each reflection, such that the combined output from the shaper contained a mix of polarization states. The degree of depolarization depended heavily upon the angle of inclination of the shaper mirrors. In one case we observed that the last row of output from the beam shaper was vertically polarized, having undergone a net 90° rotation of its polarization vector during its path through the beam shaper. In general the reflection of a beam at a surface will introduce a phase shift between the component of the beam polarized parallel and orthogonal to the plane of reflection. Hence the incremental phase shift from each reflection will fall to zero when the polarization vector of the beam lies entirely in the plane of reflection. Therefore, to maintain the polarization of the pump, we inserted a zero-order half-wave plate (WP1) before the beam shaper to rotate the polarization vector into the plane of reflection, such that phase shifts were eliminated. A second wave plate (WP2) after the shaper rotated the polarization vector back into the horizontal plane.

The output from the diode bar left the beam shaper appearing as though it was produced from an array of emitters. An image of the beam-shaped output immediately after the beam shaper in the case of the 12×5 arrangement is shown in Fig. 3. The profile was produced by imaging the output onto a CCD camera with a single achromat lens, hence the image is inverted about the x and y axes. The bottom row was therefore formed by light undeviated by the beam shaper, while the top row of output was produced by the light undergoing 11 pairs of reflections between the beam-shaper mirrors. It can be seen that light from five distinct emitters can be identified in each row, except in the top rows where the extra path length caused the output to be poorly focused at the CCD camera. It can also be seen that the smile of the diode bar produced variable amounts of dead space between consecutive rows.

Beam profiles were also taken of the pump spot close to the focal plane identified at $z=0$ in Fig. 2 by placing the CCD camera directly into the beam at the desired location. Figure 4 shows profiles for the 12×5 arrangement at 2 mm intervals along the optical axis. For each beam profile, graphs of the intensity distribution through the center of the pump spot, along the x and y axes, are also included. At $z=0$ the focused spot can be seen to be almost square. Away from the focal plane the output became rectangular in profile as the beam diverged more rapidly in the horizontal plane due to the poorer beam quality along the x axis.

The profiles shown in Fig. 4 were used to determine the 4σ dimensions of the pump spot at positions about the focus. Figure 5 shows how the focused output from the 12×5 beam-shaping arrangement corresponded to a beam with beam quality parameters $M_x^2=79$ and $M_y^2=29$.

The beam shaper was configured for three different output arrangements, giving three, four, and five columns of output. In each case the beam quality parameters M_x^2 and M_y^2 were determined. The pump power after the beam shaper was also measured in each case to determine the power transmission T. The beam quality parameters and the power transmission could be combined to determine the figure of merit F [from Eq. (2)] and the effective figure of merit F' [Eq. (3)] for each output arrangement. Table 1 summarizes the results from the three configurations investigated.

It can be seen from Table 1 that the power transmission T dropped as the number of columns of output produced by the beam shaper was reduced. The cause of the fall in power was found to be from the clipping of the beam as it passed the edges of the shaper mirrors, rather than through lossy reflections at the mirrors. The beam quality parameter M_x^2 also dropped as the number of columns of output was reduced, a trend that would be expected from fewer diode emitters contributing to the divergence in each row. It is possible that the beam quality was also af-

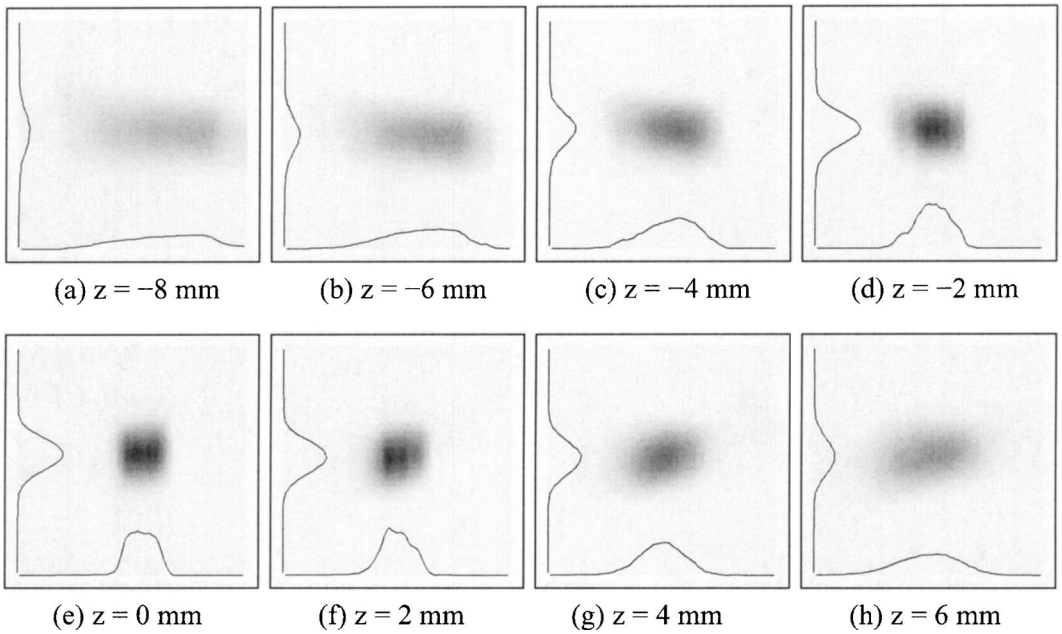

Fig. 4. Profiles of a pump spot formed by the 12×5 output in the region about focus. Each image is for a 1.95 mm×1.95 mm area of the CCD.

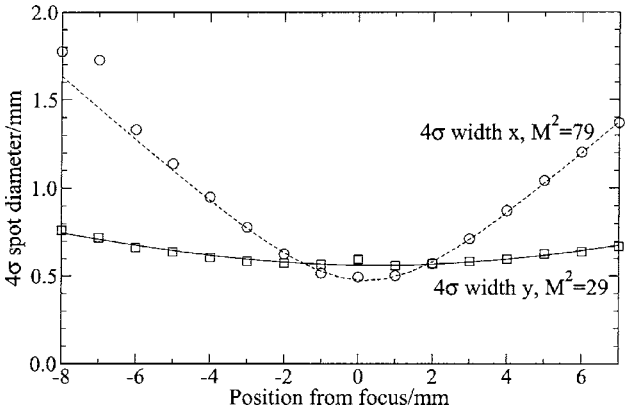

Fig. 5. Plot of 4σ measurements for a pump spot about the focus from a 12×5 output arrangement. Quadratic best-fit curves determined the M^2 values in each plane.

Table 1. Output from Beam Shaper for Different Configurations[a]

Output Format	M_x^2	M_y^2	T (%)	F	F'
60×1 (est.)	≈20	≈120	<50	$<2\times10^{-4}$	$<4\times10^{-5}$
20×3	34	29	50	5.1×10^{-4}	4.3×10^{-4}
15×4	39	19	61	8.2×10^{-4}	4.0×10^{-4}
12×5	79	29	74	3.2×10^{-4}	1.2×10^{-4}
1×60 (est.)	≈1680	≈2	100	$\approx3\times10^{-4}$	$\approx4\times10^{-7}$

[a] M^2 values are for focused pump output after shaping. Transmission T is a fraction of diode power measured after shaper versus before shaper. Also shown are the figure of merit $F=T/M_x^2M_y^2$ and effective figure of merit $F'=T/(M_{\text{worst}}^2)^2$ for the beam-shaped output. Estimated values for an unshaped bar (1×60) and a completely reformatted bar (60×1) are included for comparison.

fected by some clipping of the more divergent components of the pump beam as it passed through the beam shaper and focusing optics. The values of M_y^2 are large for both the 12×5 and the 20×3 arrangements, indicating that overly generous amounts of dead space were introduced between each row of output in both cases. Note, however, that the effective figure of merit did not depend upon M_y^2 since M_x^2 was larger for all beam-shaper configurations. The highest effective figure of merit was given by the 20×3 arrangement. Note that no further benefit would have been achieved with smaller numbers of columns of output, since for both 30×2 and 60×1 arrangements M_y^2 would exceed M_x^2.

4. MULTIPASS PUMPING OF Yb:S-FAP

We used the 15×4 beam-shaped diode output arrangement to pump a Yb:S-FAP laser. Yb:S-FAP has an absorption band at 900 nm of width 3 nm ($\sigma_p=8.6\times10^{19}$ cm^{-3} for π polarization) and a long storage lifetime of 1.26 ms, making it well suited to diode pumping.[13] There are two possible laser transitions: 985 nm (three-level, σ polarized) and 1047 nm (quasi-four-level, π polarized). We are interested in driving the three-level laser transition to obtain the fourth harmonic at 246 nm. This is a suitable wavelength for producing fiber Bragg gratings and sits between the wavelengths of two popular sources: 244 nm for frequency-doubled argon-ion lasers and 248 nm for KrF excimer lasers. We have been developing our system to lase on the quasi-four-level Yb:S-FAP transition as a first step toward obtaining output from the three-level transition, since the smaller lower-level population of the quasi-four-level transition allows the threshold for lasing to be reached more readily.

Diode-pumped laser output on the 1047 nm transition in Yb:S-FAP has been achieved by several means. End-pumped systems have been constructed by focusing the output from a stack of 22 laser diode bars into a crystal rod through a lens duct, yielding 43% slope efficiency,[14] and by focusing the output of a single-emitter laser diode into a Yb:S-FAP crystal to give 78% slope efficiency.[15] Alternatives to end-pumping methods have also been inves-

tigated, using prismatic side pumping with three laser diode bars[16] (8% slope) and multipass side pumping[17] with two laser diode bars (14%). To our knowledge, the system reported here is the first technique to end pump with a single laser diode bar.

Because of the low distribution coefficient of 12% for Yb^{3+} doping in S-FAP,[18] the concentrations possible are low compared with those in other hosts. Yb:YAG, for instance, can have up to 100% doping.[19] Electron probe microanalysis measurements of the Yb:S-FAP crystals used in our experiments gave a dopant concentration of 0.19% by weight (2.7×10^{19} cm^{-3}). The long absorption length $[N_0\sigma_p]^{-1}=4.3$ mm makes single-pass pumping inefficient for short crystals. It also prevents on-axis double-pass pumping since unabsorbed pump signal returning to the diode will seed the diode's output spectrum into the wings of the Yb:S-FAP absorption peak.

To avoid feedback we reimaged the pump spot with a pair of lenses and focused the rectangular-shaped beam to produce a square pump spot in the Yb:S-FAP crystal slightly off axis. This design is shown in Fig. 6. A plane mirror (M2) immediately behind the crystal sent the pump through the crystal a second time, so that the unabsorbed pump beam emerged from the focusing lens (SA3) at a position below the incoming pump. A right-angle prism then sent the pump back through the system for two more passes (P1). Depending upon the dimensions of the pump beam at the focusing lens, it is possible that additional prisms (a second prism is indicated in Fig. 6) could provide further passes. Shown in the left inset in Fig. 6 is a diagram of the rectangular pump beams as they appeared on the focusing lens. The rectangular far-field profile of the shaped diode output was stacked several times within the area of the lens, in an analogous fashion to the geometric multiplexing of multiple diode bars.[20] The first two pump passes were closest to being on axis, and they combined to form an approximately square profile at the focusing lens so that the spot formed by the two passes had symmetrical beam quality. The multipassing arrangement therefore dictated our choice of beam-shaper configuration, as shown in Table 1. Although the 20×3 configuration gave the highest effective figure of merit, the 2:1 ratio in the M^2 parameters of the 15×4 configuration allowed a more efficient stacking of the pump passes.

The near-hemispherical laser cavity was arranged at right angles to the pump optics by means of a high-reflector mirror (M1) with a laser-machined 45° hole through which the laser mode passed. This arrangement allowed us to use broadband reflective mirror coatings rather than the dichroic coatings required for a collinear pump–laser system. The laser cavity was formed by a plane mirror (M2) with a a broadband high-reflection coating and an output coupler that was coated for 98% reflection at the laser wavelength. The laser spot diameter at the plane cavity mirror was 325 μm, while the pump spot diameter was approximately 480 μm. The minimum pump intensity required to reach transparency on the quasi-four-level laser transition has been measured[21] to be $I_{\min}=0.09$ kW cm^{-2}, which for the given pump spot size is well within the powers available from the laser diode bar.

The Yb:S-FAP laser crystal was 1.6 mm long and was located close to the plane cavity mirror. The crystal axis was in the horizontal plane, orthogonal to the axis of the laser cavity. The incident pump radiation was therefore π polarized as perceived by the laser crystal, so that the absorption cross section was maximized. The crystal face

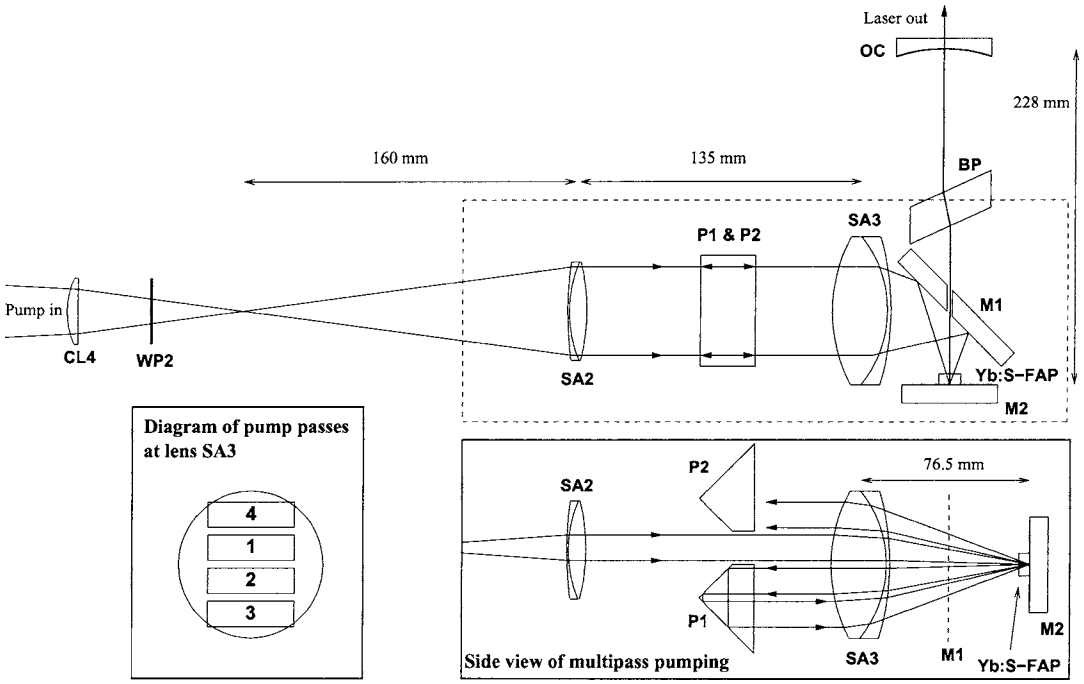

Fig. 6. Multipass pumping arrangement using beam-shaped diode output. SA2 ($f=160$ mm) and SA3 ($f=76.5$ mm): spherical achromats. P1 and P2: truncated right-angle prisms. M1 and M2: broadband highly reflective plane mirrors. OC (radius of curvature of 250 mm): output coupler. BP: Brewster plate. Inset on the right shows a side view of the pumping arrangement, unfolded about mirror M1. Inset on the left shows the pump beams at lens SA3, as viewed down the optical axis.

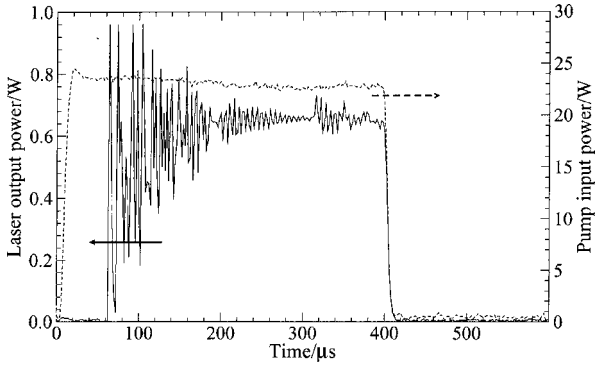

Fig. 7. Example of laser action at 1047 nm, showing photodiode traces of pump and laser signals.

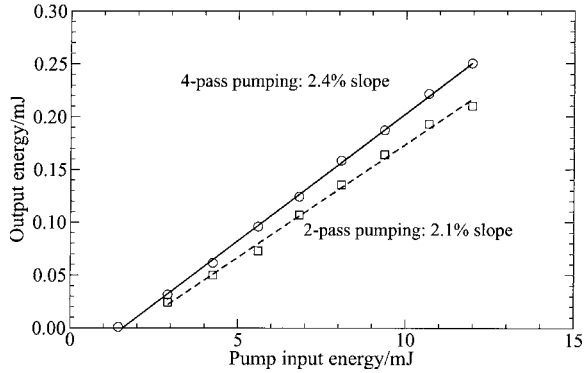

Fig. 8. Laser output energies at 1047 nm for double-pass and quadruple-pass pumping. The pump ran in quasi-cw mode, with 400 μs pulses at 35 Hz.

nearest the plane mirror was uncoated, while the other face was coated for low reflection at the pump and laser wavelengths. The uncoated face of the laser crystal was aligned parallel to the plane cavity mirror, so that losses due to reflections out of the cavity from the uncoated face were minimized. To reduce the sensitivity of the resulting etalon formed between the uncoated crystal face and the plane cavity mirror, the crystal was positioned a small distance away from the end of the cavity.

The laser cavity also contained a Pockels cell cut at Brewster's angle for the laser wavelength. The cell was used as a Brewster plate for the purposes of these investigations, thereby acting as a loss mechanism for σ-polarized radiation within the cavity. The Brewster plate suppressed parasitic lasing on the three-level laser transition, since that transition favors laser action with σ polarization.

The laser diode bar was run in quasi-cw mode, delivering pulses of 400 μs duration with a maximum peak power of approximately 24 W at the laser crystal. Figure 7 shows the typical output signal produced by the laser diode. Gain-switched output at 1047 nm was produced by the laser, after a delay of 60 μs from the start of the pump pulse. The laser signal is also shown in Fig. 7. The laser output was approximately quasi-cw in nature, with relaxation oscillations causing rapid spiking. The output appeared to be TEM_{00} in nature. However, two further sets of relaxation oscillations, at $t=190$ μs and $t=310$ μs, appear to have been caused by higher-order transverse modes developing within the cavity over the period of the pump pulse. The secondary oscillations were stable from pulse to pulse. Small changes to the alignment of the cavity caused the observed laser output to switch to higher-order modes, and these changes were accompanied by a shorter buildup time for the secondary oscillations.

Output energies were measured for the Yb:S-FAP laser for a range of pump pulse energies. Figure 8 shows laser energies achieved for two configurations: first when no prisms were used to recycle the unabsorbed pump, giving two pump passes through the laser crystal; and second when a single prism (P1 in Fig. 6) was used to provide four pump passes through the crystal. Note that the third and fourth pump passes suffered from clipping losses of approximately 40% at the focusing lens. We achieved an efficiency of 2.1% for two pump passes through the laser crystal and 2.4% with four pump passes. The threshold pump energy appears to be unchanged for two and four pump passes.

5. DISCUSSION

The effective figure of merit of the unshaped laser diode bar was estimated to be approximately 4×10^{-7}. From Table 1 it can be seen that the shaper configurations used therefore offered significantly greater figures of merit, and therefore higher effective brightness values, despite transmission losses of up to 50%. The transmitted power dropped significantly as the number of columns of output was decreased, and it is clear that the standard single-column configuration used for the two-mirror beam shaper would be unsuitable for the high fill-factor diode bar we have used. Improved results might be expected if smile could be eliminated, and with better far-field output from the diode in the y axis.

With the inclusion of the two $\lambda/2$ wave plates, shown in Fig. 2, the polarization of the pump beam can be retained, making the two-mirror beam-shaping system a suitable option for reformatting a pump source for an anisotropic laser crystal.

Beam-shaping systems are often designed to produce a symmetric beam such that the beam quality parameters are equal. In the case of the diode bar used here, symmetric output could not be achieved by producing a single column of output; the 20×3 arrangement produced the most symmetrical output in the results presented here. A fully symmetrical beam will not necessarily give the highest effective brightness when losses within the beam shaper are taken into account. It can be seen from Table 1 that both the 12×5 and the 15×4 arrangements produced beams of equivalent effective brightness, despite the beam quality parameters of the 15×4 arrangement differing by a factor of 2.

The asymmetry of the pump beam was beneficial to the multipass pumping system shown in Fig. 6, since higher asymmetry in the pump beam allows a greater number of pump passes through the laser crystal. The multipassing occurs in the direction of lowest M^2, and the effective pump profile at the focusing lens, initially rectangular for a single pass, becomes something more like a square. Hence the effective M^2 in this direction will be close to the value in the other direction. Since we are constrained by

the larger of the two values, this is an effective method to increase the brightness of the pump spot.

The multipass pumping system is similar to the system described by Giesen *et al.*,[22] which multipassed the circular output from a fiber-pigtailed diode bar. In the system presented here, however, the pump passes form a linear stack rather than a circular array, such that there is no change in effective brightness for each pass aside from the loss in power due to absorption and scattering.

The 1047 nm output from the Yb:S-FAP laser achieved a low efficiency for double-pass pumping of 2.1%, partly due to the low pump absorption of the crystal. The 1.6 mm crystal used was only 37% of the calculated absorption length for Yb:S-FAP at the peak absorption wavelength. In practice the absorption was much lower, since the emission bandwidth of the pump exceeded the bandwidth of the absorption feature in Yb:S-FAP. Single-pass absorption was measured to be approximately 10% at the start of each pump pulse. Bleaching of the ground-state Yb^{3+} population and possible sweeping of the pump wavelength over the duration of the pump pulse yielded a pulse-averaged single-pass absorption of 3%. It would therefore be preferable to make many more passes of the pump to increase the absorbed fraction of the pump.

The maximum pump intensity delivered to the laser crystal was approximately 27 kW cm^{-2}, although only a fraction of this intensity was available at the absorption peak in Yb:S-FAP. Even so, it can be seen from Fig. 7 that the laser was pumped well above threshold over the duration of each pump pulse, hence the pump intensity at the absorption wavelength must have exceeded the threshold value of 0.09 kW cm^{-2}. Improvements to the absolute efficiency of the laser could therefore be expected for a longer laser crystal, which would give greater pump absorption and increased single-pass gain on the laser transition.

Assuming 6% absorption of the pump for two passes, the slope efficiency of the laser with respect to absorbed energy was approximately 35%. Although the efficiency was higher than for side-pumped systems,[16,17] it was somewhat short of the 43% efficiency achieved by pumping with a laser diode stack[14] and significantly less than the 78% obtained by pumping with a single-emitter laser diode.[15] The efficiency of the laser was limited by losses at the uncoated face of the laser crystal. Further optimization of the output coupling may also yield significant improvements to the efficiency of the system. An optimal end-pumping configuration would also require the pump spot to have the same radius as the laser mode within the laser crystal.[7] In the system described here the pump spot was approximately 50% wider than the laser mode. As a consequence a substantial fraction of the absorbed pump energy was not extracted by the laser, reducing the slope efficiency of the laser with respect to absorbed energy. An increased mode overlap might also improve the beam quality of the laser, since less absorbed energy would be available to higher-order transverse modes.

Increasing the number of pump passes in our system from two to four achieved only a 14% improvement in absolute efficiency, with little change in the threshold pump energy. The 2:1 ratio in the beam quality parameters of the pump beam meant that only two pump passes could be stacked together without increasing the effective brightness of each pass. Hence the third and fourth passes were less effective in pumping the laser crystal on axis. The improvement in output efficiency may therefore have been due to an increase in power in the higher-order transverse modes of the laser. To increase the efficiency of the pump it would be preferable to use a more asymmetric beam. It is interesting to note that the multipass pumping system is well suited to the output characteristics of a single-emitter laser diode. The natural asymmetry of the output from a single emitter might allow it to achieve more than ten pump passes in this multipass system. Such an approach would allow efficient pumping in laser crystals with long absorption lengths.

6. CONCLUSION

Using suitable beam-shaping techniques, a high fill-factor laser diode bar containing many emitters can be used to end pump a solid-state laser. The effect of beam shaping can be described in terms of effective brightness, which is dependent upon the beam quality of the source in the direction of maximum divergence. To maximize the effective brightness of a beam-shaped source, it can be better to produce an asymmetric beam to increase the transmitted power.

We have demonstrated an asymmetric configuration of a Clarkson and Hanna-style two-mirror beam-shaping system, producing several columns of output. The simple addition of two $\lambda/2$ wave plates ensures that the polarization of the pump is retained, making the output suitable for pumping anisotropic laser crystals. The beam-shaping system was used to optically transform the output from a laser diode bar, containing a row of 60 emitters, into several output configurations. We found the best output, as characterized by effective brightness, to be an array of 20 rows of 3 emitters, giving beam quality parameters of $M_x^2=34$ and $M_y^2=29$. The effective brightness of the beam was a factor of 10^3 higher than for the output of the unaltered diode bar.

We have also presented a new multipass pumping arrangement for high brightness pumping of an optically thin gain medium, which makes efficient use of an asymmetric pump beam to allow several passes of the pump without reducing the effective brightness of each pass. The 15×4 output from the beam-shaped laser diode bar was used in the multipass pumping arrangement to end pump a Yb:S-FAP laser. Laser operation on the quasi-four-level laser transition at 1047 nm was achieved, with a slope efficiency of 2.4%. A longer crystal would give higher absorption and would yield a higher slope efficiency.

ACKNOWLEDGMENTS

This work was funded by the Engineering and Physical Sciences Research Council. We thank Colin Webb for his support in this work.

D. Coutts is available for correspondence at dcoutts@ics.mq.edu.au.

REFERENCES

1. W. A. Clarkson and D. C. Hanna, "Two-mirror beam-shaping technique for high-power diode bars," Opt. Lett. **21**, 375–377 (1996).
2. J. R. Leger and W. C. Goltsos, "Geometrical transformation of linear diode-laser arrays for longitudinal pumping of solid-state lasers," IEEE J. Quantum Electron. **28**, 1088–1100 (1992).
3. T. Graf and J. E. Balmer, "High-power Nd:YLF laser end pumped by a diode-laser bar," Opt. Lett. **18**, 1317–1319 (1993).
4. C. Gao, H. Laabs, H. Weber, T. Brand, and N. Kugler, "Symmetrization of astigmatic high power diode laser stacks," Opt. Quantum Electron. **31**, 1207–1218 (1999).
5. Y. Liao, K. M. Du, S. Falter, J. Zhang, M. Quade, P. Loosen, and R. Poprawe, "Highly efficient diode-stack, end-pumped Nd:YAG slab laser with symmetrized beam quality," Appl. Opt. **36**, 5872–5875 (1997).
6. S. Yamaguchi, T. Kobayashi, Y. Saito, and K. Chiba, "Collimation of emissions from a high-power multistripe laser-diode bar with multiprism array coupling and focusing to a small spot," Opt. Lett. **20**, 898–900 (1995).
7. T. Y. Fan and A. Sanchez, "Pump source requirements for end-pumped lasers," IEEE J. Quantum Electron. **26**, 311–316 (1990).
8. N. D. Vieira, I. M. Ranieri, L. V. G. Tarelho, N. U. Wetter, S. L. Baldochi, L. Gomes, P. S. F. de Matos, W. de Rossi, G. E. C. Nogueira, L. C. Courrol, E. A. Barbosa, E. P. Maldonado, and S. P. Morato, "Laser development of rare-earth doped crystals," J. Alloys Compd. **344**, 231–239 (2002).
9. W. A. Clarkson and D. C. Hanna, "Efficient Nd:YAG laser end pumped by a 20-W diode-laser bar," Opt. Lett. **21**, 869–871 (1996).
10. K. I. Martin, W. A. Clarkson, and D. C. Hanna, "High-power single-frequency operation, at 1064 nm and 1061.4 nm of a Nd:YAG ring laser end-pumped by a beam-shaped diode bar," Opt. Commun. **135**, 89–92 (1997).
11. N. U. Wetter, P. S. F. de Matos, I. M. Ranieri, L. C. Courrol, and S. P. Morato, "Single frequency, continuously diode-pumped Nd:LiY0.5Gd0.5F4 tunable, microlaser," Opt. Commun. **204**, 311–315 (2002).
12. N. U. Wetter, "Three-fold effective brightness increase of laser diode bar emission by assessment and correction of diode array curvature," Opt. Laser Technol. **33**, 181–187 (2001).
13. C. D. Marshall, S. A. Payne, L. K. Smith, H. T. Powell, W. F. Krupke, and B. H. T. Chai, "1.047-μm Yb–$Sr_5(PO_4)_3F$ energy-storage optical amplifier," IEEE J. Sel. Top. Quantum Electron. **1**, 67–77 (1995).
14. C. D. Marshall, L. K. Smith, R. J. Beach, M. A. Emanuel, K. I. Schaffers, J. Skidmore, S. A. Payne, and B. H. T. Chai, "Diode-pumped ytterbium-doped $Sr_5(PO_4)_3F$ laser performance," IEEE J. Quantum Electron. **32**, 650–656 (1996).
15. M. R. Dickinson, L. A. W. Gloster, N. W. Hopps, and T. A. King, "Continuous-wave diode-pumped Yb^{3+}:S-FAP laser," Opt. Commun. **132**, 275–278 (1996).
16. B. Pati, K. F. Wall, and K. I. Schaffers, "Laser performance of Yb:S-FAP in a prismatic side-pumping configuration," in *Advanced Solid-State Lasers*, M. E. Fermann and L. R. Marshall, eds., Vol. 68 of OSA Trends in Optics and Photonics (Optical Society of America, 2002), pp. 144–149.
17. B. Pati, Y. Isyanova, K. F. Wall, and P. F. Moulton, "Yb:S-FAP multipass side-pumped amplifier," in *Advanced Solid-State Photonics*, J. J. Zayhowski, ed., Vol. 83 of OSA Trends in Optics and Photonics (Optical Society of America, 2003), p. 197.
18. K. I. Schaffers, J. B. Tassano, A. B. Bayramian, and R. C. Morris, "Growth of Yb:S-FAP [Yb^{3+}:$Sr_5(PO_4)_3F$] crystals for the Mercury laser," J. Cryst. Growth **253**, 297–306 (2003).
19. F. D. Patel, E. C. Honea, J. Speth, S. A. Payne, R. Hutcheson, and R. Equall, "Laser demonstration of Yb3Al5O12 (YbAG) and materials properties of highly doped Yb:YAG," IEEE J. Quantum Electron. **37**, 135–144 (2001).
20. T. Y. Fan, A. Sanchez, and W. E. DeFoe, "Scalable, end-pumped diode-laser-pumped solid-state laser," Opt. Lett. **14**, 1057–1060 (1989).
21. L. D. DeLoach, S. A. Payne, L. K. Smith, W. L. Kway, and W. F. Krupke, "Laser and spectroscopic properties of $Sr_5(PO_4)_3F$–Yb," J. Opt. Soc. Am. B **11**, 269–276 (1994).
22. A. Giesen, H. Hugel, A. Voss, K. Wittig, U. Brauch, and H. Opower, "Scalable concept for diode-pumped high-power solid-state lasers," Appl. Phys. B **58**, 365–372 (1994).